Mecánica Computacional Vol. XXIII, pp. 2249-2270
G.Buscaglia, E.Dari, O.Zamonsky (Eds.)
Bariloche, Argentina, November 2004

MODELING MIXTURE FORMATION IN A GDI ENGINE

Rossella Rotondi*

* Dipartimento di Ingegneria Meccanica,Università di Roma "Tor Vergata"
Viale del Politecnico 1, 00133 Roma, Italia
e-mail: rossella.rotondi@uniroma1.it

Key words: Gasoline Direct Injection, atomization, combustion, swirl atomizer.
Abstract. *Mixture formation and combustion in a Gasoline Direct Injection (GDI) engine were studied. A swirl-type nozzle, with an inwardly opening pintle, was used to inject the fuel directly in a 4 stroke, 4 cylinder, 4 valves per cylinder engine. The atomization of the hollow cone fuel spray was modeled by using an hybrid approach validated at first in a quiescent chamber at ambient pressure and temperature, comparing numerical penetration and spray shapes with the experimental ones. For both stoichiometric and stratified operation mode the interaction of the liquid jet and the surrounding air was studied. The most important obstacle in the development of GDI engines is that the control of the stratified-charge combustion over the entire operating range is very difficult. Since the location of the ignition source is fixed in SI engines the mixture cloud must be controlled both temporally and spatially for a wide range of operating conditions. The development of a successful combustion system depends on the design of the fuel injection system and the matching with the in-cylinder flow field. Results show that the stratification at part load appears to be the most crucial and critical step, and if the air motion is not well coupled with the fuel spray it would lead to an increase of unburned hydrocarbon emission and consumption*

1 INTRODUCTION

To satisfy CO_2 emissions restrictions that will be introduced in the industrialized countries, Brake-specific fuel consumption (BSFC) has to be reduced. Gasoline port-fuel injection engine that are in production today have an higher BSFC compared to the direct-injection (DI) Diesel engine. This is due to the higher compression ratio and the unthrottled operation typical of diesel engines, that, however, have higher NO_x and soot emissions, slightly higher noise level and lower startability. The ideal would be to put together the best features of the both combining Diesel efficiency with gasoline specific power. Studies in this direction have shown that this may be achieved with gasoline direct injection (GDI) unthrottled engine[1,2]. Fuel is injected directly into the combustion chamber in order to have a mixture with an ignitable composition near the spark plug at the time of ignition for all loads. Power is controlled by varying the amount of fuel injected in a diesel-like manner, and with the unthrottled operation pumping losses are significantly reduced. Because of the charge cooling during injection, higher compression ratio, lower octane requirement and increased volumetric efficiency lead to an improved BSFC up to 30%. The critical step in the development of such engines is the stratification at partial loads, at which, an erroneous mechanism of mixture formation leads to an increase of engine specific consumption and unburned hydrocarbons emissions.

2 FUEL INJECTION SYSTEM IN GDI ENGINES

GDI injectors can either be single fluid or air-assisted (two phase) and may be classified by atomization mechanism (sheet, turbulence, pressure, cavitation), by actuation type, nozzle configuration (that can be either swirl, slit, multihole or cavity type), or by spray configuration (hollow-cone, solid-cone, fan, multi-plume). A detailed classification of GDI injectors may be found in [1]. Currently the most widely used injector for GDI applications, the one analyzed in this paper, is the single-fluid, swirl-type unit, that uses an inwardly opening pintle, a single exit orifice and a fuel pressure, in the range of 70-100 bar.

The liquid emerges from the single discharge orifice as an annular sheet that spreads radially outward to form an initially hollow-cone spray. Pressure energy is transformed into rotational momentum that enhances atomization. The initial spray angle ranges between 25°-150° and the Sauter Mean Diameter (SMD) varies from 14-23 μm. Surface roughness may, however, produce streams of fuel in the fuel sheet, resulting in formation of pockets of locally rich mixture. A schematic representation of is reported in figure 1[1].

The spray has a leading edge (the main spray tip) that penetrates away from the nozzle tip for about 50mm in less then 20ms. A Toroidal vortex is also attached to the periphery. The leading edge of the spray contains a separate sac spray.

The fuel injection system needs to provide different operating modes for the different loads. Fuel injection pressure vary in a range from 40 to 130 bar. In the full-load case a stratified homogenous charge is needed and this is done with a early injection, during the induction. A well dispersed spray is desirable, with bigger cone angle and a conical shape. At part-load, a late injection is needed in order to allow stratified charge combustion, with a well atomized compact spray to control the stratification. The fuel is injected during the compression stroke

when the cylinder pressure is about 10 bar, which requires a relatively higher injection pressure compared to the full-load case. The higher injection pressure is necessary to reduce the Sauter mean radius (SMD) of the liquid spray, because the fuel must vaporize before the spark event occurs in order to limit unburned hydrocarbons (UBHC) emissions and to have a repeatable ignition process. The smaller the droplet size the faster the vaporization occurs. GDI systems require fuel droplets of under 20 μm SMD, (Diesel engine require SMD lower than 8 μm).

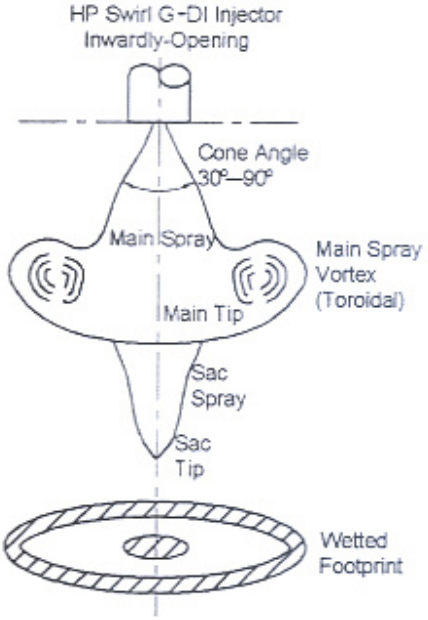

Figure 1. Schematic representation of a HP Swirl GDI Injector Inwardly opening

3 THE EXPERIMENTAL ENGINE

The numerical code has been tested comparing numerical results with experiments[3] on a GDI, 4 cylinder, 4 valves per cylinder, whose characteristics are reported in Table 1.

Table 1
Basic engine geometric characteristics

Bore	7.2 [cm]
Stroke	10.2 [cm]
Displacement	459.5 [cm^3]
Number of Cylinder	4
Compression ratio	12.5

This engine is fuelled by the injector previously described. Compared to a Multi-Point Injection (MPI) engine it is characterized by an higher compression ratio typical of this class of engines.

As load changes the combustion varies from stratified to homogeneous. The engine, as it can be evinced from the CAD design of figure 2, has in one of each cylinder's intake duct a swirl valve able to modify the air motion in the cylinder as a function of the engine operating conditions. For the full load case, requiring an homogeneous charge (stoichiometric air/fuel ratio), the above mentioned valve is completely open determining a well organized swirl motion in the cylinder, while at part load, when a stratified charge is needed, the valve is throttled in order to have a tumble motion in the chamber. In figure 2 a CAD design of the engine and the related computational grid are shown.

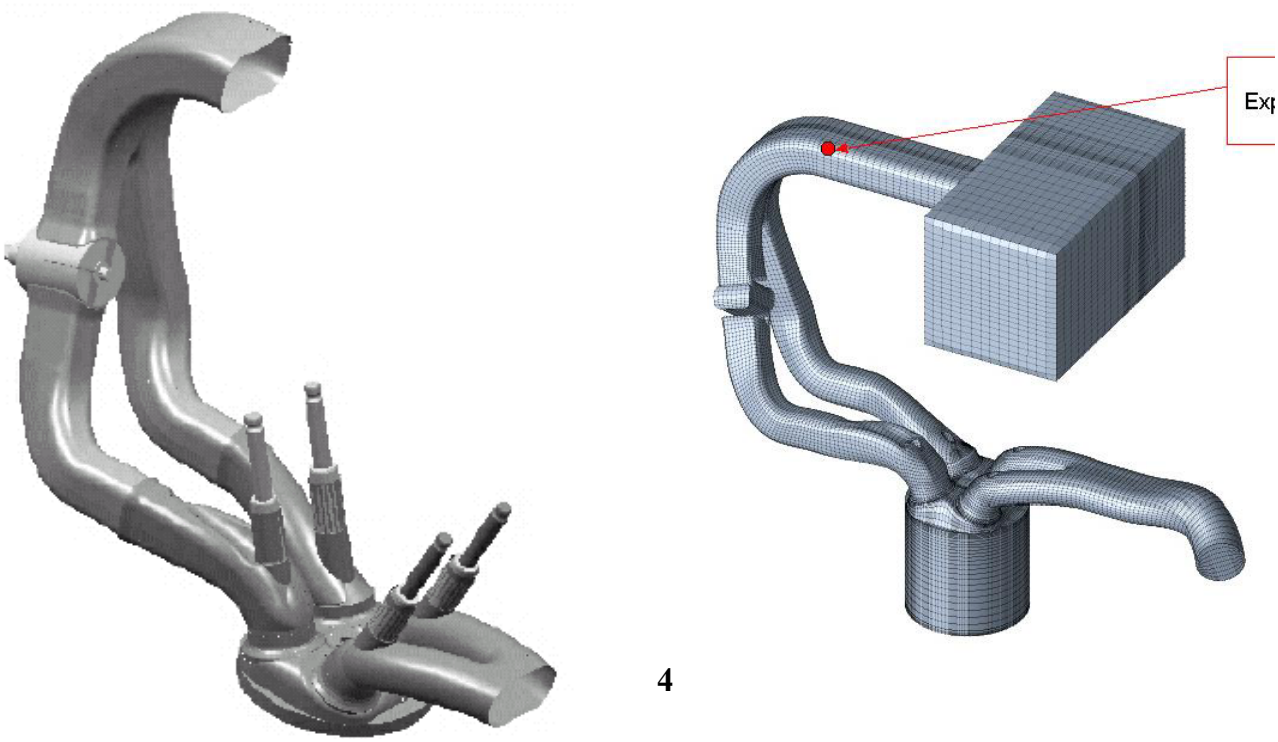

Figure 2. CAD design of the engine and related computational grid

4 NUMERICAL CODE

The developed numerical computation tool "NCF 3D" is based on the well known KIVA III code originally developed by the Los Alamos Laboratory[4,5]. The original version employs a finite volume approximation of the governing 3D Navier-Stokes (N-S) equations in a Cartesian or cylindrical reference system in which a multi-block grid structure is generated. A modified $\kappa - \varepsilon$ turbulence model, accounting for compressibility effects, is used during the Arbitrary Lagrangian Eulerian (ALE) integration of the averaged N-S equations. The original version has been enhanced by a certain number of specific submodels necessary for GDI engine modeling

as listed in the following:

4.1 Boundary Conditions – 1D Simulations

The whole engine was first simulated following a fully 1D approach[6], at different full load and part load conditions. Figure 3 shows the intake system, the plenum collector, the four cylinders and the exhaust system. Ambient conditions are set at the intake and exhaust boundaries.

Then 3D simulations, at the same load conditions, were performed, and the boundaries conditions at the inlet of the 3D domain (plenum) and the exhaust were imposed by the corresponding values in the 1D simulations.

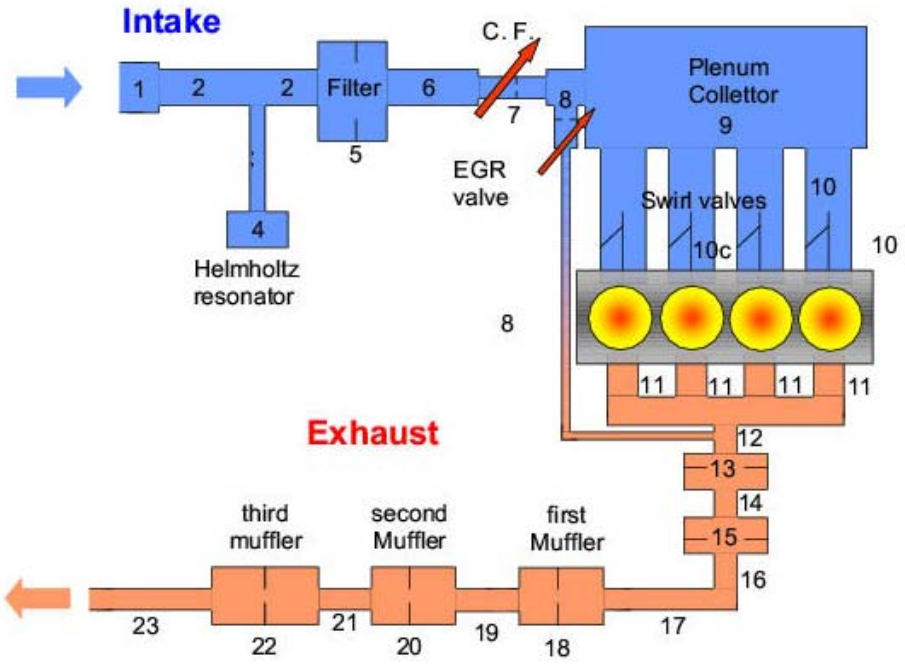

Figure 3. Schematic of the whole engine in the 1D approach

Comparisons were made between experimental pressure, the 1D and the 3D numerical one, in the intake duct, at the location shown in figure 2. The related diagrams are reported in figure 4 for a part load case (up) and a full load case (down).

It can be seen that the experimental and numerical pressure profile vs. crank angle present the same frequency while some discrepancies in the magnitude is present. This is due to the heat transfer and friction effects evaluations, but in order to provide boundary conditions to the 3D code the 1D results are acceptable, being the volumetric efficiency error lower than 10%.

Comparisons were also made between the experimental and 1D numerical pressure in the plenum, and experimental and 3D numerical pressure in the cylinder at different loads. Results show an agreement with a discrepancy of 7% in the worst case.

For the 3D simulations following cycles were also simulated in order to evaluate the influence of initial conditions. At high engine speed (up to 5000 rpm) up to 3 following cycles were simulated in order to minimize the differences. Differences were stronger for the part load cases.

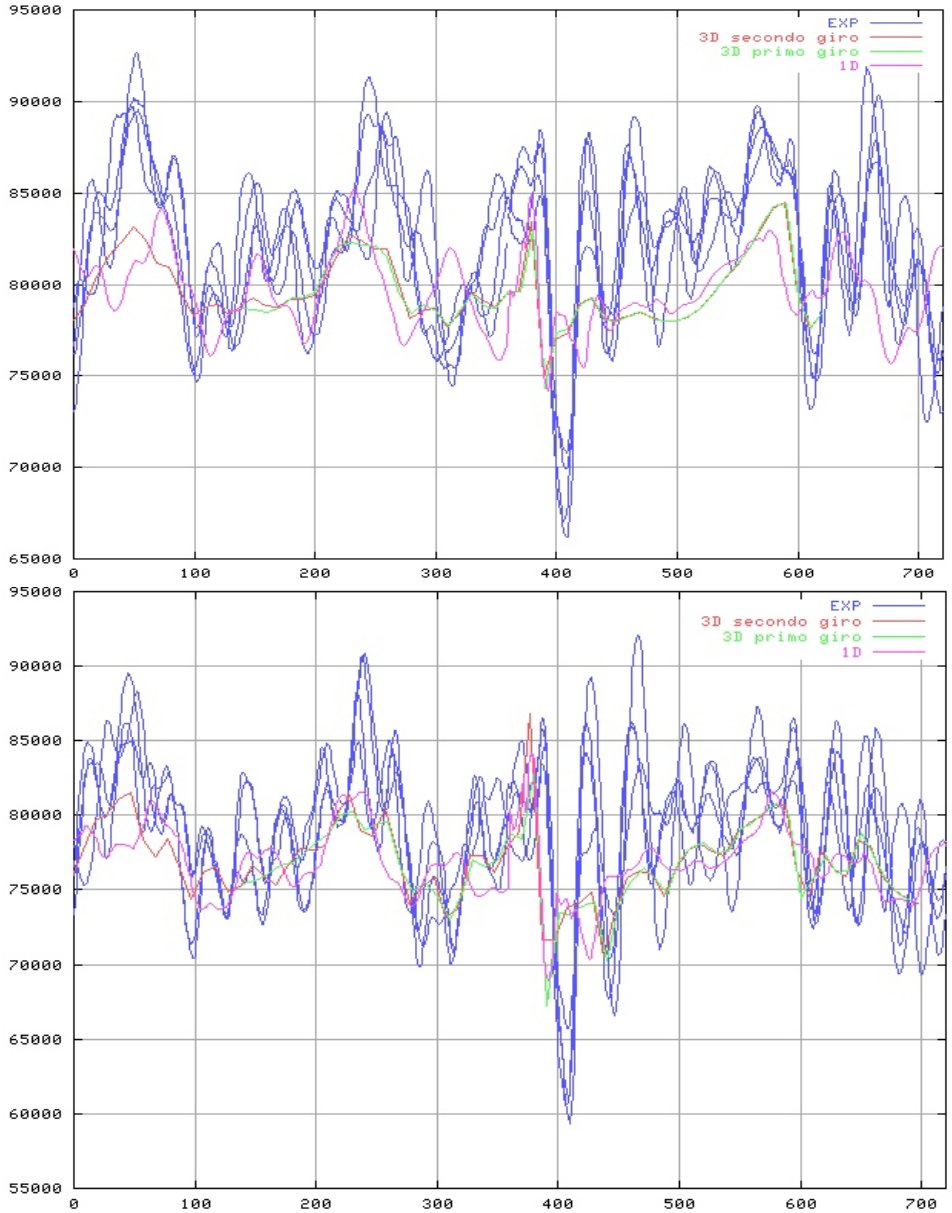

Figure 4: Comparison between numerical (1D and 3D) and experimental pressure in the intake duct. Part load case (up) and full load case (down).

4.2 Injection and Atomization models

A Lagrangian treatment of stochastic particle injection is used for the liquid drops that simulate the spray. The fuel spray enters the computational domain as an annular sheet, but in the KIVA spray model this continuous liquid is artificially divided into discrete Lagrangian parcels injected into the gas. Each computational parcel represents a group of physically similar droplets that exchange mass momentum and energy with that surrounding air through source terms in the gas phase equations. The liquid jet is simulated injecting blobs with characteristic size equal to the sheet thickness.

Following Nagaoka's approach[7] the liquid jet exiting the injector is treated as a liquid *sheet* till it reaches its breakup length. The *sheet* is analyzed discretizing its volume in small quantities and applying to them the momentum conservation equation:

$$\frac{d\bar{u}_f}{dt} = C_s \frac{\rho_g \left|\left(\bar{u}_g - \bar{u}_f\right)_n\right|}{\rho_f}\left(\bar{u}_g - \bar{u}_f\right)_n + \frac{1}{\rho_f}\frac{\partial p}{\partial n}$$

in which $\bar{u}_g$ is the velocity vector related to the gas comprehensive of the turbulence term (for which the k-ε model implemented in KIVA was used), $\bar{u}_f$ is the velocity vector related to the liquid "*sheet*". Subscript *n* refers to the sheet normal directions, *g* and *f* to gas and fluid respectively. The variation of the *sheet* thickness during the injection period, is evaluated imposing mass conservation:

$$h_f = \frac{K_0}{L + K_0 / h_0} \qquad K_0 = h_0(w_0 - h_0)\cos\theta/(2sin\theta)$$

where K_0 represents the sheet thickness variation, L the distance from the injector and θ is the angle respect to the injector axis[8]. In the previous expression h_0 represents the sheet thickness at the exit of the injector, while w_0 represents the characteristic length so it was put equal to the nozzle diameter, d_0. The breakup length is evaluated by means of the formula[9]

$$L_b = \frac{18\sqrt{2}}{F}\sqrt{\frac{\rho_f}{\rho_g}}\frac{h_f}{\sqrt{We_h}}$$

where F is the ratio between the amplitude of the pressure waves that arise in viscous flow over those in a unviscous flow. F is evaluated as follows:

$$F = \sqrt{N(2-N)}\left[\left(1+\frac{N^3V^2}{4(2-N))}\right)^{3/2} - \frac{3}{2}\sqrt{\frac{N^3V^2}{4(2-N))}}\right]$$

$$N \approx (1+2.29V)^{-0.677}$$

$$V = \frac{\sqrt{2}}{4}Z$$

$$Z = Oh \cdot We$$

$$Oh = \frac{\mu_f}{\sqrt{\rho_f \sigma_f h_f}}$$

$$We = \frac{\rho_g u_{rel}^2 h_f}{\sigma_f}$$

being u_{rel} the relative velocity between gas and liquid, σ_f the surface tension force of the liquid, μ_f the liquid viscosity. Before the droplet detaches from the liquid sheet, because of the interaction between the two phases, *ligaments* of characteristic size d_L, are formed on the surface of the conical sheet:

$$d_L = \left(\frac{8}{9}\right)^{1/3}\left[\frac{K_0{}^2\sigma_f{}^2}{\rho_g\rho_f u_{rel}{}^4}\right]^{1/6}\left[1+2.6\mu_f\left(\frac{K_0\rho_g{}^4 u_{rel}{}^7}{72\rho_f{}^2\sigma_f{}^5}\right)^{1/3}\right]^{1/5}$$

These *ligaments* detach as droplets of diameter d_D related to the *ligament* size by the following correlation:

$$d_D = 1.88 \cdot d_L \cdot (1+3 \cdot Oh_L)^{1/6} \qquad Oh_L = \frac{\mu_f}{\sqrt{\rho_f \sigma d_L}}$$

in which Oh_L is the Ohnesorge number of the *ligament*[10].
d_D is proportional to the characteristic size to be put in the Rosin-Rammler distribution function[11]

$$1 - V = e^{-\left(\frac{D^q}{\overline{D}}\right)}$$

$$\overline{D} = C_1 d_D$$

(that is widely used in spray applications), to determine the post breakup sizes of the

primary parcels. Usually for internal combustion engines applications 1.5 <q< 4, and was put equal to 3.5[12]. C_1 is an empirical factor[13], put equal to 1. In present simulation this model was used for primary atomization as done in previous work[14].

Once the droplets are formed they may undergo secondary breakup. This was modeled using different approaches in the different regimes as the droplet Weber number changes as done in previous works[15].

4.3 Combustion model

The approach used is based on a suggestion made by Abraham et al[16] and subsequently modified by Reitz[17] and is particularly suitable for GDI combustion computation in highly stratified charge conditions due to the strong influence that the value of the local air/fuel ratio exerts on the formulation of the burning rate. In this combustion model the time rate of change of the partial density of species i, due to the conversion from one chemical species to another is given by:

$$\frac{dY_i}{dt} = -\frac{Y_i - Y_i^*}{\tau_c}$$

Where $\boldsymbol{Y_i}$ is the mass fraction of species i and $\boldsymbol{Y_i^*}$ is the local and instantaneous thermodynamic equilibrium value of the mass fraction. $\boldsymbol{\tau_c}$ is defined as the characteristic time scale to achieve the equilibrium. The characteristic time scale is assumed to be the same for all the considered species. The characteristic conversion time scale $\boldsymbol{\tau_c}$ is assumed to be expressed as:

$$\tau_c = \tau_l + \tau_t$$

where $\boldsymbol{\tau_l}$ is the laminar conversion time scale and $\boldsymbol{\tau_t}$ the turbulent mixing time scale.
The characteristic laminar conversion time scale for the gasoline has been evaluated as a function of pressure $\boldsymbol{P}$, temperature $\boldsymbol{T}$ and equivalence ratio $\boldsymbol{f}$, using the procedure described in[16]. A power-law was used to determine the laminar burning velocity for the gasoline combustion in each computational cell[18]:

$$S_l = S_{lo}\left(\frac{T_u}{T_0}\right)^{\alpha}\left(\frac{p}{p_0}\right)^{\beta}$$

Where for the gasoline α, β are given by:

$$\alpha = 2.4 - 0.271\phi^{3.51} \qquad \beta = -0.357 + 0.14\phi^{2.77} \qquad S_{lo} = B_m + B_\phi(\phi - \phi_m)$$

Once the laminar burning velocity in the flame is determined, it is possible to evaluate the flame thickness and the laminar conversion time by means of the following expressions:

$$\delta_l = \frac{\overline{D}_l}{S_l} \qquad \tau_l = \frac{\delta_l}{S_l}$$

being $\overline{D}$ an average value of the laminar diffusion coefficient in the flame front.

The turbulent mixing time scale can be estimated according to Magnussen and Hjertager[19] and introducing a delay coefficient as suggested in[16,20]. The use of this coefficient takes in consideration the delay of the turbulent mixing allowing, during the delay period, the laminar flame to move a distance equal to two or three times the length scale of the turbulent eddies. The delay coefficient f can be expressed as:

$$f = -\exp\left(-\frac{t - t_s}{\tau_d}\right)$$

where: $$\tau_d = C_1 \frac{l_t}{S_l} \qquad l_t = C_\mu^{3/4} \frac{k^{3/2}}{\varepsilon \cdot \kappa}$$

with $k=0.41$ (the von Karman constant).
The turbulent mixing time scale can then be expressed as:

$$\tau_t = C_2 \frac{k}{\varepsilon} \chi \cdot f$$

where $\chi = 1$ for $h = 1$

$\chi = 1/h$ for $h \geq 1$

being

$$h = \frac{0.6(Y_p - Y_{ps})}{(Y_f - Y_f^* + Y_{02} - Y_{02}^*)}$$

where subscript p and ps refer to products of combustion at actual and stoichiometric condition respectively, and the constants Y_{ps} and Y_p are given in the table below:

Table 2.
Summary of combustion model constants

B_m	30.5
B_ϕ	-54.9
Φ_m	1.21
C_μ	0.09
C_1	8.0
C_2	0.142

4.4 Spark Plug model

A model that simulates the initial flame kernel formation and development in SI engines was used according to[21,22]. The ignition phase includes electrical discharge, plasma breakdown and shock wave propagation. The mixture in the combustion chamber is ignited by the electric discharge between the spark plug electrodes. The spark discharges the electrical energy through the arc and glow phases. Plasma is created and the flame kernel is produced by the plasma. All these phenomena occur in a very short period of time (less than 10^{-6} sec) and in a relatively small domain, which has a size ranging from the spark gap distance to the order of the turbulence integral length scale[18].

The initial temperature and diameter of the plasma are given by :

$$T_i = \left[\frac{1}{\gamma}\left(\frac{T_b}{T_0} - 1\right) + 1\right] T_0$$

$$d_i = 2\left[\frac{\gamma - 1}{\gamma}\frac{E_b}{\rho_0 d(1 - T_0/T_i)\pi}\right]^{1/2}$$

where γ is the specific heat ratio, E_b and T_b are the breakdown energy and temperature respectively, d is the gap distance between the electrodes and T_0 and p_0 temperature and pressure in the combustion chamber.

Heat is dissipated in all directions following the equation:

$$\frac{\partial T}{\partial r} = \alpha\left(\frac{\partial^2 T}{\partial^2 r} + \frac{2}{r}\frac{\partial T}{\partial r}\right) + \frac{\eta_{B,G} U(t) I(t) + E_{che}}{\rho_{pl} c_p V_k}$$

with the following initial conditions:

$$T(0,r) = T_i \qquad \text{if } 0 < r < d_i/2$$

$$T(0,r) = T_0 \qquad \text{if } r > d_i/2$$

in which α is the thermal diffusivity, ρ_{pl} is the gas density of plasma, c_p the specific heat at constant pressure, $I(t)$ and $U(t)$ current and voltage as measured across the spark gap and $\eta_{B,G}$ the energy transfer efficiency for arc and glow discharge respectively given by the following expression[22]:

$$\eta_{B,G} = \eta_{0B,G} + \frac{(\eta_{\infty B,G} - \eta_{0B,G})U^3}{A_{B,G} + U^3}$$

in which $\eta_{0B,G}$ and $\eta_{\infty B,G}$ are the energy transfer efficiency for a quiescent mixture and for very high velocities (v>>15 m/s) respectively. $A_{B,G}$ are given constants (see table 3) and U is the voltage as measured across the spark gap.

Table 3
Spark model constants

Parameter	Arc discharge	Glow discharge
η_{0B}	36	8
η_{∞}	50	30
A(m/s)	500	700

Kernel radius r_k is then determined as the location at which the temperature equals the adiabatic flame temperature. The kernel velocity v_k is then calculated as the time derivative of r_k. Two distinct transition criteria can be used to switch from the ignition model to the combustion model. The one proposed by Herweg and Maly[22] states that the ignition process should be finished when the kernel velocity reaches the laminar burning velocity. Another criteria proposed by Reitz et al.[23] imposes the kernel size to reach the order of the integral length scale:

$$d_k \geq C_k l_T$$

where C_k=*3.5* and l_T is the turbulence length scale related to the turbulent kinetic energy, k, and its dissipation rate, ε, by:

$$l_T = 0.16 \frac{k^{1.5}}{\varepsilon}$$

5 NUMERICAL RESULTS AND COMPARISON WITH EXPERIMENTAL DATA

5.1 Spray simulations

In a previous work[24] the atomization model was tested comparing numerical and experimental data. Tests were made injecting gasoline in a quiescent chamber (1 bar pressure, 300K temperature). Such conditions, if besides the absence of a well developed flow field, are

not that far from the in-cylinder ones since the injection starts during the intake stroke and the beginning of compression.

The spray is of a hollow cone type and the injector is fuelled by a displacement pump that compresses the fuel up to 100 bar. For the tests a computational grid of 3mm spacing was used. The results are presented in terms of comparison between the numerical and experimental tip penetration and a comparison of the spray morphology at different time steps. The tip penetration is determined by the pre-spray that is injected with a very small cone angle compared to the maximum value (90°) and with a value of velocity near to the maximum. The variation of spray cone angle and injection velocity are evaluated experimentally and given to the code as spray model initial conditions. Comparing numerical and experimental tip penetration (figure 5) it is evident how the code well predicts this macroscopic quantity. Initially they both have a linear trend which becomes parabolic due to the drag effects, subsequently the atomization of the sheet produces many small droplets increasing the exchange surfaces between air and liquid. All this phenomena are well modeled determining a discrepancy between the numerical and experimental values of less then 2%.

In figure 6, the overlay of numerical and experimental spray images is reported. The experimental pictures are obtained by means of a CCD camera synchronized with a laser light pulse at different time steps. All the images show a good correlation between the numerical and experimental spray. The breakup length at which the primary blobs start to breakup can be noticed. The evolution of the pre-spray is very important in determining the penetration. From the figures, at the latest time steps, small secondary droplets at the periphery of the jet can be noticed. These are characterized by small diameter and Weber number and are like floating in the surrounding air and are carried up by the flow field.

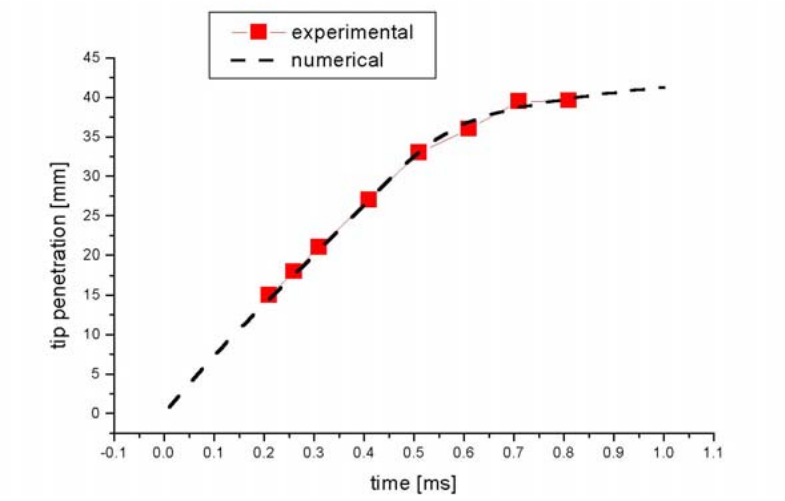

Figure 5. Numerical and experimental tip penetration versus time

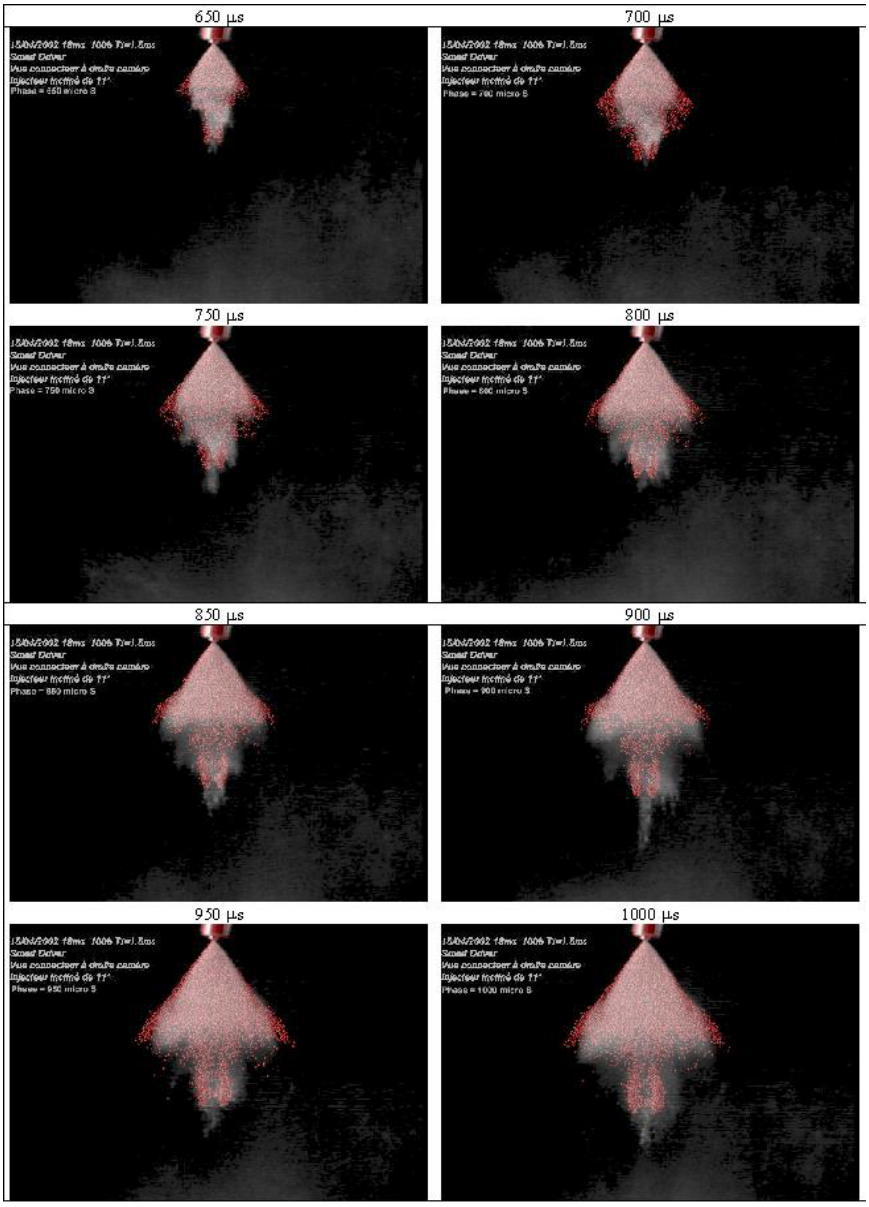

Figure 6. Experimental and Numerical Spray morphology

5.2 Engine simulations

To correctly predict the combustion phase a precise mixture formation modeling is absolutely necessary, so present simulation must involve also the intake and exhaust stroke to have a right prediction of the air motion inside the cylinder which highly influences the mixture formation.

The grid generation is generated within the main frame of the original design in CAD-CATIA , while the final multi-block mesh for the KIVA III solver is made by the IBM created

interface, the ENGAGE code. The resulting computational domain was shown in figure 2. The grid has about 160.000 computational cells and discretizes the cylinder and part of the intake and exhaust systems.

Different simulations were performed at different loads (from 0 to 6 bar mean effective pressure, mep) and engine speed (from 750 to 5000 rpm), different EGR, for homogeneous and stratified charge cases. Homogeneous mixture in this kind of engine is a globally stoichiometic mixture with a local non homogeneity that can go up to about 5%. This produces significant variations in ignition delay and in unburned hydrocarbons emission. Locally rich zones can give, for this kind of engines, soot emissions

For the homogeneous case results concerning the configuration shown in table 4 will be presented. In figure two plots of the lambda distribution are reported in different planes. It can be seen how the mixture is nearly homogeneous around the stoichiometric value (lambda=1).

Table 4
Operating condition for the homogeneous case

	Rpm	Mep	EGR	Lambda	Spark advance
Case 0	3000	6 bar	10 %	0.954	21.4°

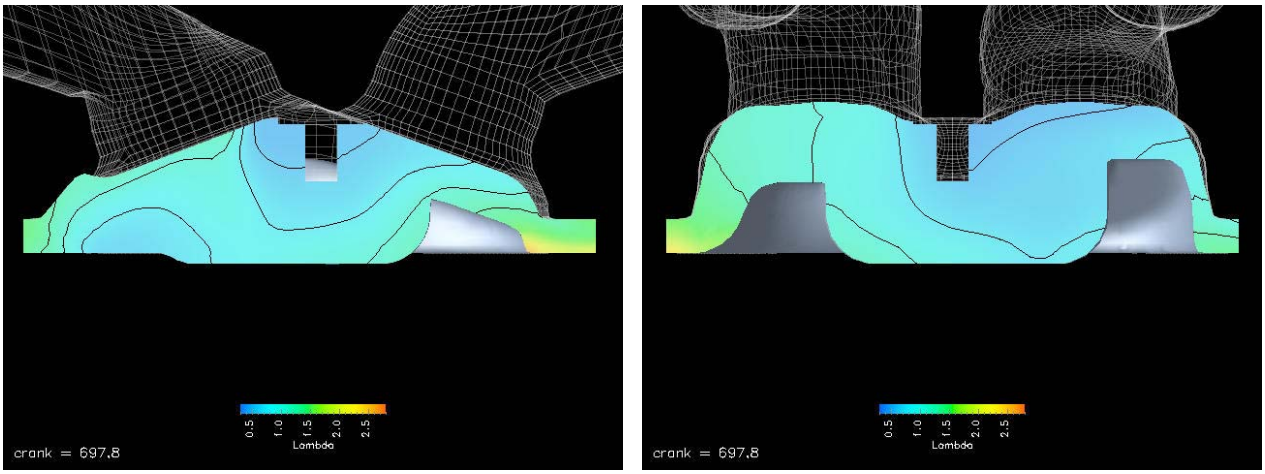

Figure 7: Lambda distribution in the combustion chamber. Homogeneous case

To test the predictive capability of the spark model several simulation were performed for this case varying the spark advance timing and comparing numerical results with experiments. In the following picture the experimental indicated cycle of the engine was compared to the numerical one for the following spark timing: 21.4° (nominal) 29°, 27°, 25°, 24°, 22°, 17°, 12°, 7°, 4°, 1°, -2°. In the following simulation the model constants were set for the nominal spark advance timing and never changed. The experimental curves are an average of 64 consecutive cycles. As it can be seen in most cases four experimental diagrams are

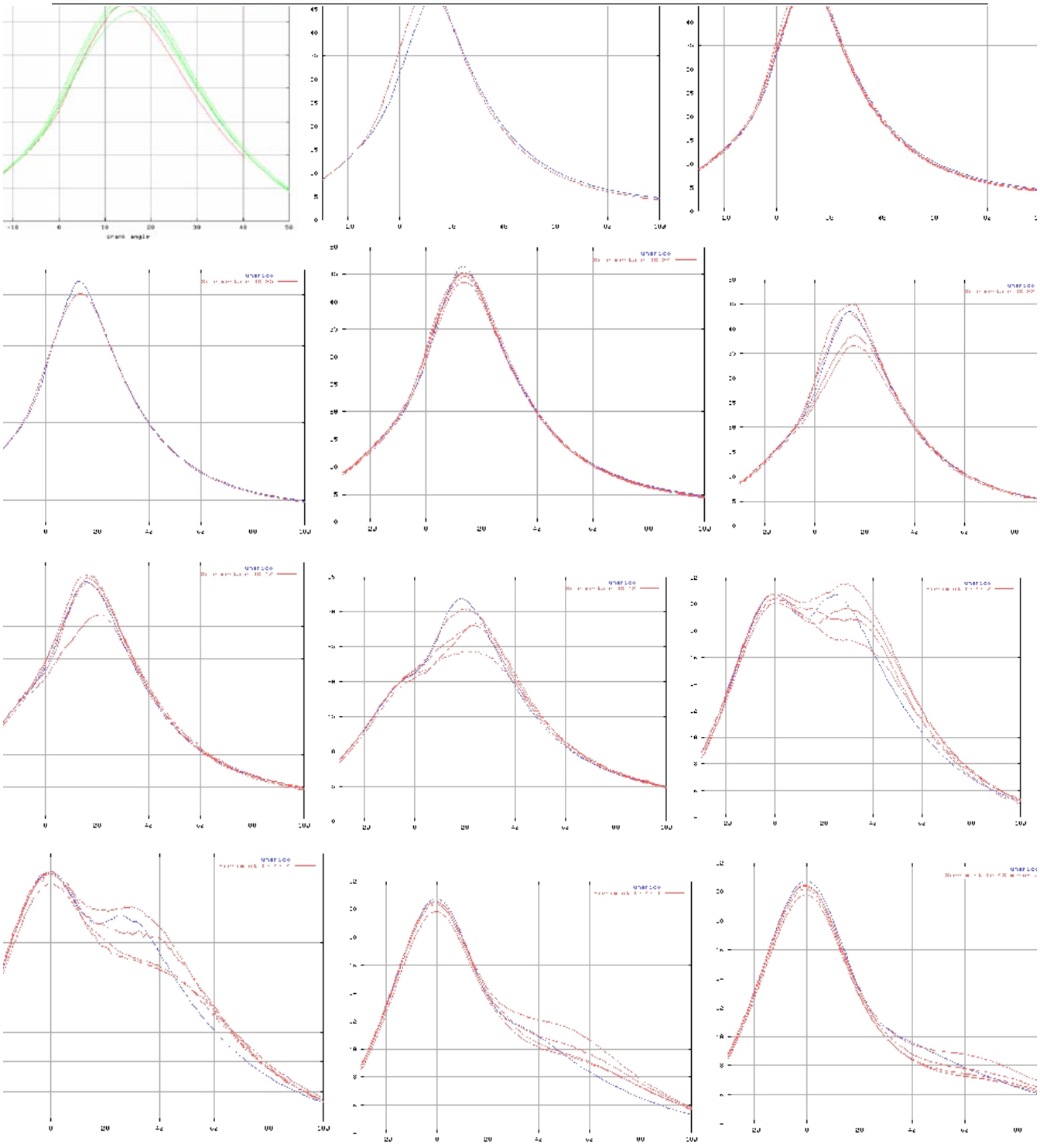

Figure 8: Indicated cycle for different crank timing: 21.4° 29°, 27°, 25°, 24°, 22°, 17°, 12°, 7°, 4°, 1°, -2°

shown and this because in some operating conditions there were big differences between the 4 cylinders. This is probably due to the plenum particular shape. The numerical cycle was acceptable if laying between the four experimental ones. The results show very good agreement, if not considering the second plot (29° spark advance). Being this case very stable (the four cylinders have the same history) this could be due to an erroneous modeling of the ignition process since, because of the shorter time from the start of injection, air/fuel mixture present strong gradients near the plug.

As mentioned before, for GDI engines, the most challenging problem is the charge stratification and combustion at part load, so results concerning some cases in the stratified mode will be presented in the following, as listed in table 5. As it can be evinced from the table the part load cases with higher EGR are reported. These are certainly the most difficult one since there is little fuel that needs a very high stratification of the charge, made harder by the high levels of EGR.

Table 5
Operating conditions of 3 different cases.

	Rpm	Mep	EGR	Lambda	Spark advance	Injected mass	Start of injection
Case1	1000	4 bar	15%	1.477	18.9	12.94 mg	637.2°
Case2	2000	4 bar	10%	1.58	22.1	12.73 mg	626.6°
Case3	2000	2 bar	20	2.072	24.1	8.150 mg	638°

As it can be evidenced in the following figures the volume of the spark was considered when discretizing the computational domain. This is fundamental in GDI engine modeling since the volume occupied by the spark plug is not neglectable being it much bigger than the ones used in port fuel injection engines. Figure 9 shows on the left hand side the lambda distribution when the spark volume is considered and it is much different from the one we have on the right hand side in which the same case, but in a grid in which this volume is neglected, is reported.
The reason for this completely different air-fuel distribution is that the tumble motion, that determines the mixing, is different in the two cases. If not considering the plug, the tumble in a vertical plane through the cylinder axis has a characteristic length equal to half the combustion chamber, but if the plug is considered this characteristic length is the half of the previous one. Instead of having one big vortex, in a vertical plane, we have two distinct tumble motions on each side of the chamber and this can be seen in a second cloud of fuel in the left side of the chamber completely absent in the second picture.

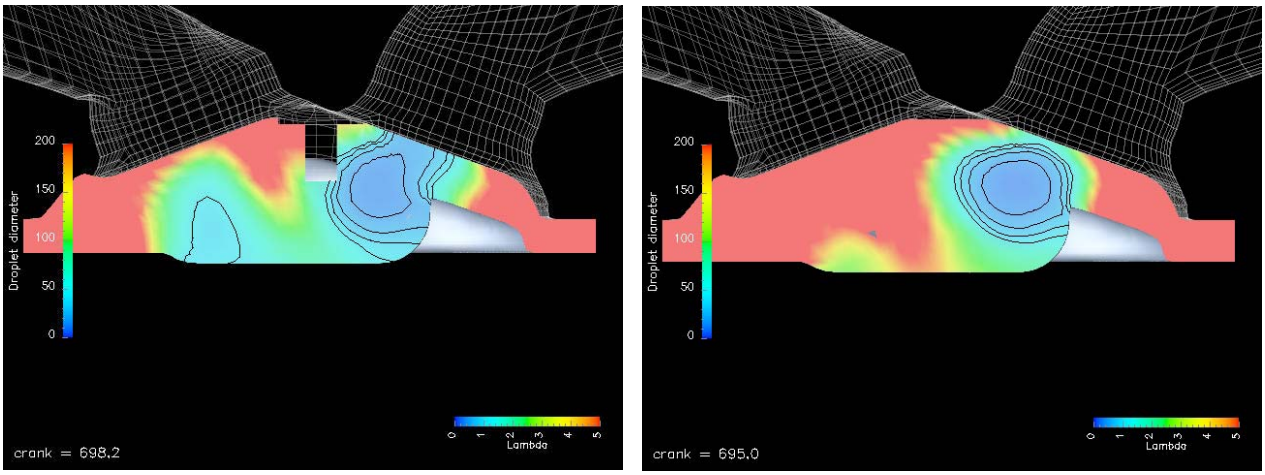

Figure 9: Lambda distribution. Case3. Grid considering the volume of the plug (left), grid neglecting it (right)

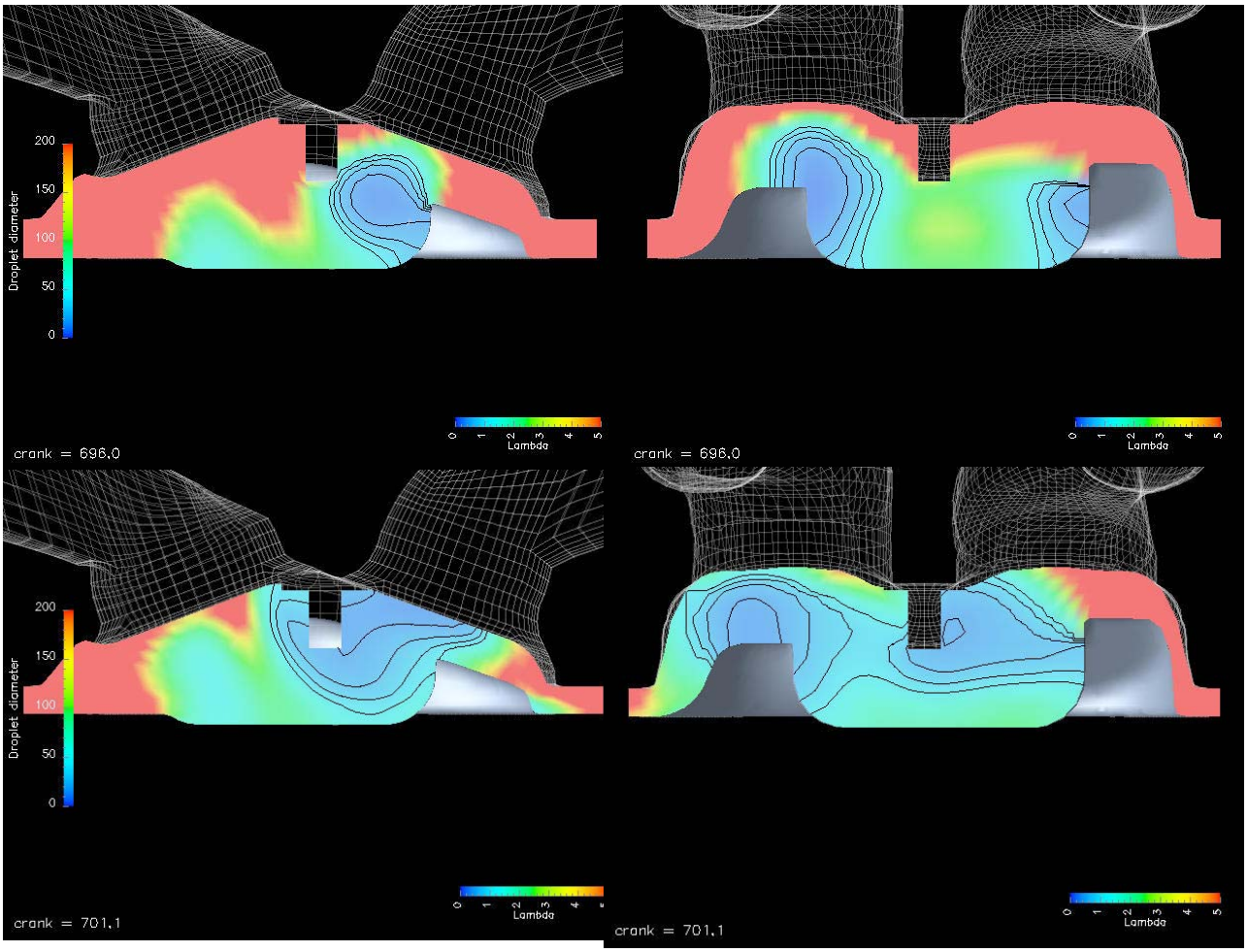

Figure 10: Lambda distribution. Case1 (up) and case 2 (down) in two different planes

In figure 11 pressure is plotted against crank angle, comparing the experimental (in each of the four cylinder) and numerical one for the 3 cases.

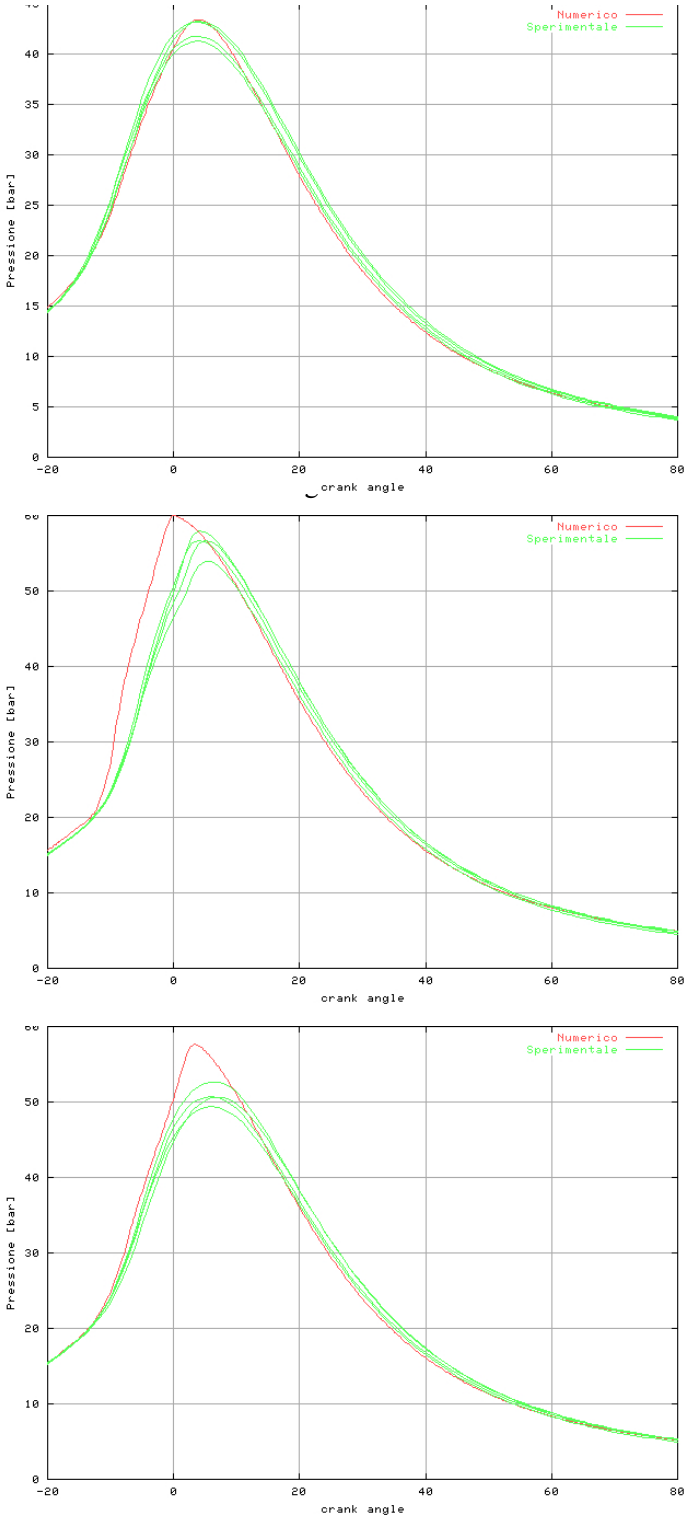

Figure 11: Indicated cycle for the 3 cases

6 CONCLUSIONS

[1,2],Mixture formation and combustion in a 4-stroke, 4-cylinder, 2 valves per cylinder Gasoline Direct Injection Engine fuelled by a swirl injector with a inwardly opening pintle, was studied.

At first a 1D simulation of the whole engine was performed in order to provide more realistic boundaries conditions to the NCF-3D code. Both stratified charge (at part load) and nearly homogeneous (at higher loads) were modeled for different engine speeds and different percentage of EGR. Stratified charge is obtained at part load by throttling a swirl valve in one of the two intake ducts of each cylinder. This determines a tumble motion in the chamber that helps in the formation of a stratified mixture near the spark plug. A modified ignition model was used and tested varying the spark advance timing in the homogeneous case. Results show good agreement. Results also show that the spark plug, which is an internal obstacle, may effect the in-cylinder flow field and the subsequent mixture formation, especially at part load. Therefore the plug volume was considered when generating the computational grid.

The numerical results globally show that the stratification at part load is the most crucial and critical step, and if the air flow motion is not well coupled with the fuel spray, the combustion could be not complete with higher exhaust emissions.

7 REFERENCES

1. F.F. Zhao, D.L. Harrington, M.C. Lai, Automotive Gasoline Direct-Injection Engines, SAE, 2002

2. F.Q. Zhao, M.C. Lai, D.L. Harrington, A review of Mixture Preparation and Combustion Strategies for Spark-Ignited Direct Injection Gasoline Engine, SAE 970627

3. Nu.M.I.D.I.A Private Communications, 2003

4. A.A. Amsden, J.D.Ramshaw, P.J.O'Rourke, J.K. Dukowicz, A Computer Program for two and three Dimensional Fluid Flows whit Chemical Reaction and fuel Spray, Los Alamos Labs., LS 12503 MS, 1993;

5. A. Amsden, KIVA-3: A KIVA Program with Block-Structured Mesh for Complex Geometries", Los Alamos National Laboratory, 1993

6. Marco Alessandri, "Simulazione della fase di ricambio della carica in un motore benzina ad iniezione diretta" Tesi di Laurea Università di "Tor Vergata", 2000

7. Nagaoka M., Kawamura K., A deforming Droplet Model for Fuel Spray in Direct-Injection

Gasoline Engines, SAE 2001-01-1225, 2001

8. Dombrowski N., Hasson D., Ward D, Chem Engr. Sci., 12, pp35-50, 1960

9. Dombrowski N., Johns D., The aerodynamic instability and disintegration of viscous liquid sheets, Chem Engr. Sci., 18, pp203-214, 1963

10. Ohnesorge, W., Formation of Drops by Nozzles and the Breakup of Liquid Jets, Z. Angew. Math. Mech., Vol. 16, 1936, pp. 355—358

11. Sauter, J., Determining Size of Drops in Fuel Mixture of Internal Combustion Engines, NACA TM 390, 1926

12. Z. Han, S. Parrish, P.V. Farrel, R. D. Reitz, Modeling Atomization Processes of Pressure Swirl Hollow-Cone Fuel Sprays, Atomization and Sprays, vol.7, pp.663-684, 1997.

13. Hayakawa, M., Takada, S., Yonesige, K. Nagaoka, M., Takeda, K., Fuel Spray Simulation of a Slit Nozzle Injector for Direct-Injection Gasoline Engine, SAE 2002-01-1135, 2002

14. Beccaria, M., Bella, G., Lanzafame, R., Simulazione Fluidodinamica di uno Spray di Combustibile per Motori ad Accensione Comandata GDI, ATI 2003

15. R. Rotondi, G. Bella, C. Grimaldi, L. Postrioti, Atomization of High-Pressure Diesel Spray: Experimental Validation of a New Breakup Model, SAE Paper 2001-01-1070,2001

16. Abraham J., Bracco F.V., Reitz R.D. "Comparison of Computed and Measured Premixed Charge Engine Combustion" Combustion and Flame 60: pp 309-322, 1985

17. Reitz, R. D., Kuo T. W. ;"Modelling of HC Emissions Due to Crevice Flows in Premixed Charge Engines" SAE Paper 892085

18. Heywood J. B. "Internal Combustion Engine Fundamentals." Mc-Graw Hill Book Co, New York, 1995

19. Magnussen B. F., Hjertager B. H.; Sixteenth Symposium (International) on Combustion, The Combustion Institute Pittsburgh 1971 pp 649 – 657

20. Reitz, R.D., "Assessment of Wall Heat Transfer Models for Premixed-Charge Engine Combustion Computations" SAE Paper 910267

21. Jeonghoon Song, Myoungho Sunwoo, “A Modeling and Experimental Study of Initial Flame Kernel Developement and Propagation in SI Engines”, SAE Paper 2000-01-0960R.

22. Herweg and R. R. Maly, “A Fundamental Model for a Flame Kernel Formation in S.I. Engines”, SAE Paper 922243

23. L. Fan, G. Li, Z. Fan, R. D. Reitz, “Modeling Fuel Preparation and Stratified Combustion in a Gasoline Direct Injection Engine”, SAE Paper 1999-01-0175

24. Gino Bella, Rossella Rotondi, “Gasoline Direct Injection Spray Simulation”, CHT-04 Paper number CHT-04-166